UNCECOMP 2023
5th ECCOMAS Thematic Conference on
Uncertainty Quantification in Computational Sciences and Engineering
M. Papadrakakis, V. Papadopoulos, G. Stefanou (eds.)
Athens, Greece, 12—14 June 2023

ROBUST PROBABILITY BOUNDS ANALYSIS FOR FAILURE ANALYSIS UNDER LACK OF DATA AND MODEL UNCERTAINTY

Adolphus Lye[1,4], **Ander Gray**[2,4], **Marco de Angelis**[3,4], **and Scott Ferson**[4]

[1] Singapore Nuclear Research and Safety Initiatives, National University of Singapore, Singapore
e-mail: snrltsa@nus.edu.sg

[2] United Kingdom Atomic Energy Authority, United Kingdom
e-mail: ander.gray@ukaea.uk

[3] University of Strathclyde, United Kingdom
e-mail: marco.de-angelis@strath.ac.uk

[4] Institute for Risk and Uncertainty, University of Liverpool, United Kingdom
e-mail: {adolphus.lye, akgray, mda, ferson}@liverpool.ac.uk

Keywords: Interval arithmetic, Probability box, Bayesian inference, Transitional Ensemble Markov Chain Monte Carlo, Adaptive pinching, Model uncertainty, Dependence.

Abstract. *The paper serves as a response to the recent challenge problem published by the NAFEMS Stochastic Working Group titled: "Uncertain Knowledge: A Challenge Problem" whereby the participants are to implement current practices and 'state-of-the-art' stochastic methods to address numerous uncertainty quantification problems presented in the challenge.*

In total, two different challenge problems on increasing complexity levels are addressed through the use of the following techniques: 1) Bayesian model updating for the calibration of the distribution models and model selection for the aleatory variables of interest; 2) Adaptive-pinching method for the sensitivity analysis; and 3) Probability Bounds Analysis to quantify the uncertainty over the failure probabilities.

For the reproducibility of the results and to provide a better understanding of the numerical techniques discussed in the paper, the MATLAB and R codes implemented to address the challenge problems are made available via: `https://github.com/Institute-for-Risk-and-Unce`
`NAFEMS-UQ-Challenge-2022`

1 Introduction

Currently, one of the biggest challenge faced in the design of critical engineering systems is the lack of available data. As such, this introduces a significant degree of uncertainty in this aspect and therefore the need to employ uncertainty quantification tools which are robust under little information. In general, such uncertainties can be group into two distinct categories: 1) Aleatory uncertainty; and 2) Epistemic uncertainty [1, 2]. The aleatory uncertainty stems from the inherent variability of the system and is/are usually modelled as random variable(s) following a distribution function. Such uncertainty is irreducible. The epistemic uncertainty, on the other hand, stems from the lack of knowledge over the system and is represented by a fixed value within a bounded set which reflects the level of knowledge over the parameter(s) of interest. Unlike aleatory uncertainties, epistemic uncertainties are reducible through the process of improving knowledge such as data-collection [3].

To provide such settings where both of such uncertainties exist and need to be quantified, the NAFEMS Stochastic Workings Group (SWG) has recently published a challenge titled: "Uncertain Knowledge: A Challenge Problem" [4] which will be tackled in this paper. Details to the challenge problems are also provided in Sections 3 and 4 of the paper. For each of the challenge problems presented, the objectives are the following:

1. To quantify the uncertainty over the failure probability P_f due to limited data;
2. To determine the variable which contributes most to the uncertainty in the prediction of P_f; and
3. To determine a value of P_f used to make a decision on the engineering system of interest.

The structure of the paper follows as such: Section 2 provides descriptions of the UQ methods that will be employed to address the challenge problems, Section 3 provides the approach towards addressing Challenge problem 1, Section 4 provides the approach towards addressing Challenge problem 2, and Section 5 summarises the content presented and drawing the paper to a close.

2 Research Methodologies

This section presents detailed descriptions to the various methodologies that are implemented to address the problems presented in the NAFEMS challenge. Detailed explanations to the approaches can be found in the respective references.

2.1 Bayesian Model Updating

A well-known stochastic model calibration approach is the Bayesian model updating technique which is based upon Bayes' inference [5, 6]:

$$P(\boldsymbol{\theta}|\boldsymbol{D}, M) = \frac{P(\boldsymbol{D}|\boldsymbol{\theta}, M) \cdot P(\boldsymbol{\theta}|M)}{P(\boldsymbol{D}|M)} \tag{1}$$

whereby $\boldsymbol{\theta}$ represents the vector of inferred parameter(s), $\boldsymbol{D}$ represents the vector of observed data, M represents the model that is being considered for updating, $P(\boldsymbol{\theta}|M)$ represents the prior, $P(\boldsymbol{D}|\boldsymbol{\theta}, M)$ represents the likelihood function, $P(\boldsymbol{\theta}|\boldsymbol{D}, M)$ represents the posterior, and $P(\boldsymbol{D}|M)$ is the model evidence term or the normalising constant to ensure that $P(\boldsymbol{\theta}|\boldsymbol{D}, M)$ integrates to 1. Detailed explanations to each of the above terms are found in [6].

In the context of the challenge questions, $\boldsymbol{\theta}$ is used to represent the inferred shape parameters of the distribution model M (i.e. Normal, Exponential, Beta, etc.) associated with the aleatory variable based on the limited data $\boldsymbol{D}$ provided.

2.1.1 Transitional Ensemble Markov Chain Monte Carlo

In general, $P(\boldsymbol{\theta}|\boldsymbol{D}, M)$ is not normalised due to the complexity in computing $P(\boldsymbol{D}|M)$. To sample from the un-normalised $P(\boldsymbol{\theta}|\boldsymbol{D}, M)$, numerous Markov chain based advanced sampling techniques have been developed [6]. For this work, the recently-developed Transitional Ensemble Markov Chain Monte Carlo (TEMCMC) sampler is implemented given it is the "state-of-the-art" technique used for Bayesian model updating. It needs to be highlighted, that one can also implement relatively simpler MCMC techniques such as Gibbs sampling and Metropolis-Hastings sampling. Based on the Transitional Markov Chain Monte Carlo concept, it samples from $P(\boldsymbol{\theta}|\boldsymbol{D}, M)$ through a series of "transitional" distributions P^j [7]:

$$P^j \propto P(\boldsymbol{D}|\boldsymbol{\theta}, M)^{\beta_j} \cdot P(\boldsymbol{\theta}|M) \tag{2}$$

where j is the iteration number taking integers from 0 to m, and β_j is the tempering parameter such that $\beta_0 = 0 < \beta_1 < \cdots < \beta_{m-1} < \beta_m = 1$. Full details to the TEMCMC sampler and its algorithm are found in [8].

There are two key reasons for implementing TEMCMC sampler in this set of challenge problems: 1) it is robust in sampling from complex-shaped posteriors indirectly though the use of P^j; and 2) it is able to compute $P(\boldsymbol{D}|M)$ which is a metric used to rank different models M based on the observed data $\boldsymbol{D}$. The TEMCMC sampler computes the evidence $P(\boldsymbol{D}|M)$ by evaluating the mean of the sample nominal weights across iterations and then multiplying them together [7, 6]. This makes the TEMCMC sampler applicable in performing Bayesian model selection under model uncertainty (i.e. see Challenge problem 2 in Section 4).

2.1.2 Approximate Bayesian Computation

To perform Bayesian inference on $\boldsymbol{\theta}$, the Approximate Bayesian Computation (ABC) approach is employed [9]. To do so, an approximate Gaussian likelihood function is used [10]:

$$P(\boldsymbol{D}|\boldsymbol{\theta}, M) \propto \exp\left(-\frac{d}{\epsilon}\right)^2 \tag{3}$$

where d is the stochastic distance metric, which in this case quantifies the degree of similarity between the Empirical Cumulative Distribution Function (ECDF) of the given data $\boldsymbol{D}$ and the chosen distribution model of the aleatory variable, while ϵ is the width factor of the approximate Gaussian function. In this case, the stochastic area metric is chosen as the stochastic distance metric defined as:

$$d = \int_{-\infty}^{\infty} |F_D(x) - F_M(x)| dx \tag{4}$$

where F_D denotes the CDF of the empirical data $\boldsymbol{D}$, while F_M denotes the CDF of the distribution model M, e.g. Normal distribution, that is to be updated. Further mathematical details can be found in [11]. To allow for an acceptable degree of precision on the computation of d whilst ensuring computational efficiency, 100 samples are drawn from F_M to construct its ECDF.

There are two key reasons to justify the use of the stochastic area metric: 1) it is a non-parametric metric as there is no need for the user to define a tuning parameter such as the bin-width in the case of the Bhattacharyya distance [10]; and 2) it can be implemented along ECDFs which is particularly useful especially if the data-size is small and its true distribution profile cannot be simply determined from its histogram.

2.2 Adaptive-pinching Method

Part of the analysis in this challenge involves determining the aleatory variable which contributes most to the uncertainty on the failure probability P_f. To achieve this, a sensitivity analysis is performed on the inferred parameters defined by $\boldsymbol{\theta}$ to quantify and rank these parameters according to their sensitivity on the P_f interval denoted as Δ. Such analysis will be done using the Adaptive-pinching method which provides a non-empirical approach to determine the pinched bounds of a chosen inferred parameter which yields the greatest reduction in Δ [12].

The procedure to the method is as follows: For a chosen variable θ^{n_d}, for $n_d = 1, \ldots, N_d$ is the component index of $\boldsymbol{\theta}$, its given interval is divided into 10 equally-spaced sub-intervals. At iteration $j = 1$, the first sub-interval is isolated and serves the the "pinched" space. This is done whilst keeping the remaining interval of the $N_d - 1$ component(s) unchanged. From which, the computation of P_f is performed accounting for the "pinched" interval of θ^{n_d}. Denoting the resulting reduced interval of P_f as Δ_p, the sensitivity index Ω for the chosen θ^{n_d} is defined [13]:

$$\Omega = 1 - \frac{\Delta_p}{\Delta_0} \tag{5}$$

whereby Δ_0 is the initial interval on P_f before the adaptive-pinching procedure. After this is done, the analysis and computation of Ω is repeated for iterations $j = 2$ to $j = 10$ from which, the maximum value of Ω is determined among the 10 iterations. This maximum value of Ω achieved by θ^{n_d} will be its sensitivity score. The procedure is then repeated for the remaining $N_d - 1$ variable(s). An illustrative description to the above procedure is provided in Figure 1.

From the analysis, aleatory variable whose inferred distribution shape parameter has the highest value of Ω will be reflected as the variable which contributes the most to the uncertainty on P_f.

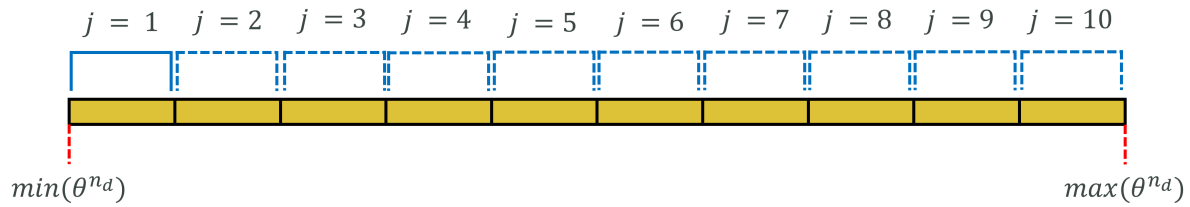

Figure 1: Illustration to the Adaptive-pinching approach for the Sensitivity analysis.

3 Challenge Problem 1

3.1 Problem Description

In this problem, two aleatory variables are presented: R and S whose respective data are presented in Table 1. It is stated that both R and S follow a Normal distribution which is assigned as the model M to be updated for both aleatory variables. From there the corresponding limit state function g is defined as:

$$g = R - S \tag{6}$$

while the failure probability P_f is defined as:

$$P_f = P(g < 0) \tag{7}$$

Based on the available information and data on R and S, the uncertainty on P_f needs to be quantified.

To address the problem, Probability Bounds Analysis (PBA) is implemented [14]. In doing so, it will not be assumed that R and S are independent and that the uncertainty over the dependency between the two aleatory variables will be accounted for in the uncertainty quantification of P_f.

$R\,[MPa]$	503.252	460.005	485.503	466.061	475.449	–	–	–	–	–
$S\,[MPa]$	376.594	278.222	331.535	330.774	395.173	394.203	387.309	361.754	300.191	381.090

Table 1: Table of data for R and S.

3.2 Results and Discussions

3.2.1 Model Calibration

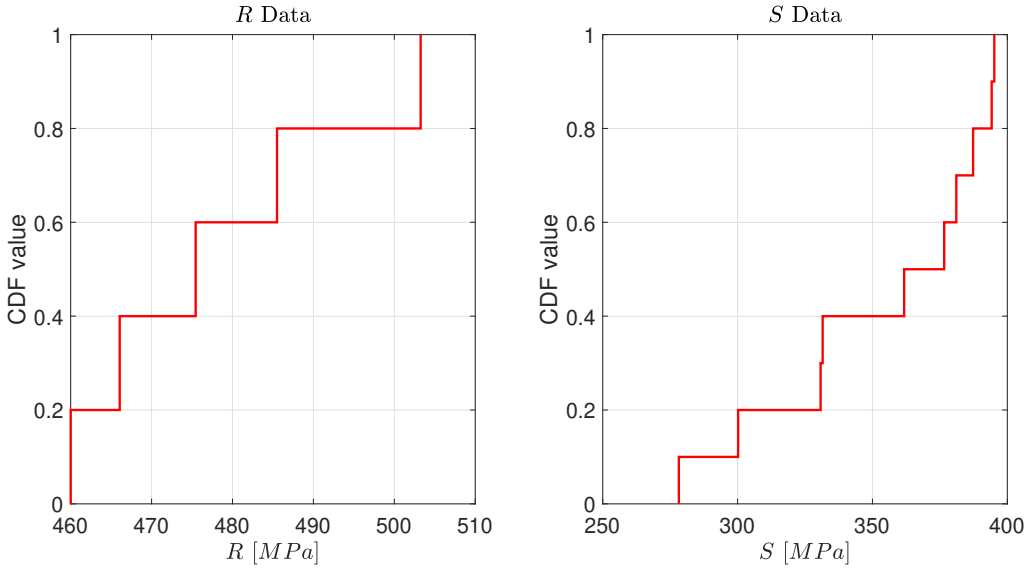

Figure 2: ECDF of R and S based on the numerical data in Table 1.

Figure 2 presents the respective ECDF plots for R and S from which, the Bayesian model updating approach is implemented to infer the following Normal distribution shape parameters for R and S: $\boldsymbol{\theta}_R = \{\mu_R, \sigma_R\}$ and $\boldsymbol{\theta}_S = \{\mu_S, \sigma_S\}$ respectively. Details to the respective inferred parameters are found in Table 2.

For each inferred parameter, a Uniform prior is assigned whose corresponding bounds are defined in Table 2. The likelihood function used is the approximate Gaussian function defined in Eq. (3).

To infer $\boldsymbol{\theta}_R$, the width parameter of the likelihood function is set at $\epsilon = 5.0$. The same setting is used when inferring $\boldsymbol{\theta}_S$ This is to ensure: 1) a sufficient degree of convergence on the posterior $P(\boldsymbol{\theta}|\boldsymbol{D}, M)$; and 2) to ensure an acceptable number of iterations (i.e. between 5 to 6) by the TEMCMC sampler so as to keep computational costs relatively low.

$\boldsymbol{\theta}$	Description	Prior bounds	Units
μ_R	Mean of R	$[300, 600]$	$[MPa]$
σ_R	Standard deviation of R	$[5, 100]$	$[MPa]$
μ_S	Mean of S	$[200, 500]$	$[MPa]$
σ_S	Standard deviation of S	$[5, 100]$	$[MPa]$

Table 2: Details to the respective inferred parameters and the corresponding prior bounds.

The resulting sample histogram obtained from $P(\boldsymbol{\theta}|\boldsymbol{D}, M)$ for the respective inferred parameters are presented in Figure 3. From which, credible intervals at different levels $L_c \in [0, 100]$ $\%$ could be obtained. The choice of L_c for the respective inferred parameters is presented in Table 3 along with their resulting interval bounds. The justification behind the the corresponding values of L_c used is to ensure the tightest possible resulting P-box for R and S whilst ensuring they enclose the ECDFs shown in Figure 2. The resulting P-boxes for R and S are presented in Figure 4.

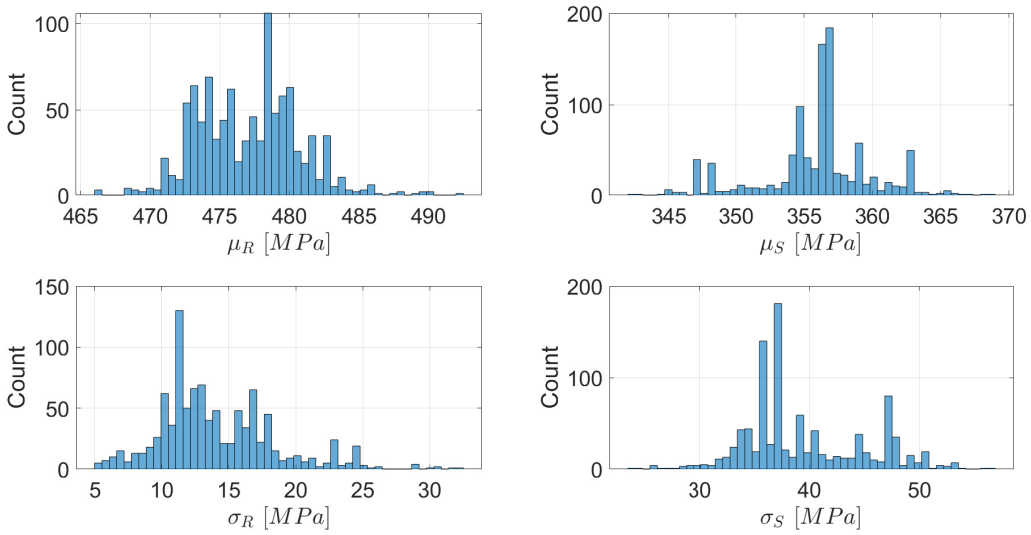

Figure 3: Histogram of the posterior samples for $\boldsymbol{\theta} = \{\mu_R, \sigma_R, \mu_S, \sigma_S\}$.

$\boldsymbol{\theta}$	L_c $[\%]$	Interval	Units
μ_R	5.0	$[471.7296, 482.5105]$	$[MPa]$
σ_R	5.0	$[8.0288, 23.0162]$	$[MPa]$
μ_S	0.0	$[342.1467, 368.6816]$	$[MPa]$
σ_S	0.0	$[23.6986, 56.7473]$	$[MPa]$

Table 3: Results to the L_c and the resulting interval for the respective inferred parameters.

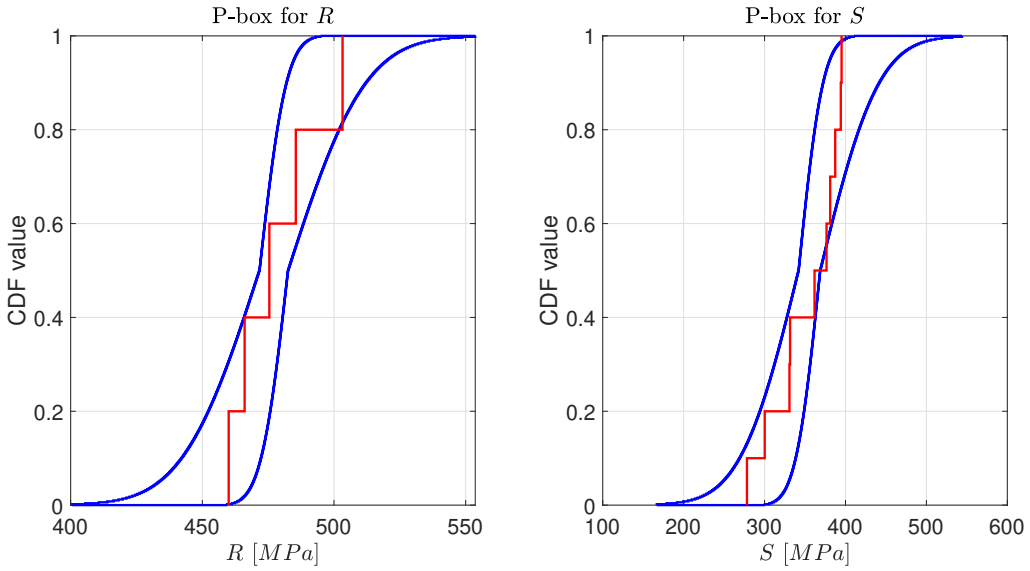

Figure 4: Resulting P-box obtained for R and S (in blue) along with their respective ECDFs of the observed data (in red).

From the resulting P-boxes obtained for R and S, the P-box for g is obtained based on Eq. (6) and presented in Figure 5. As such, based on Eq. (7), we obtain the following results for P_f summarised in Table 4. As seen in the results in Table 4, the upper-bound on P_f is higher when considering the uncertainty over the dependency between R and S. To provide a conservative yet robust decision by accounting for such uncertainty, the reference value will be set at $P_f = 0.1760$ which will be used for decision-making over the system in question.

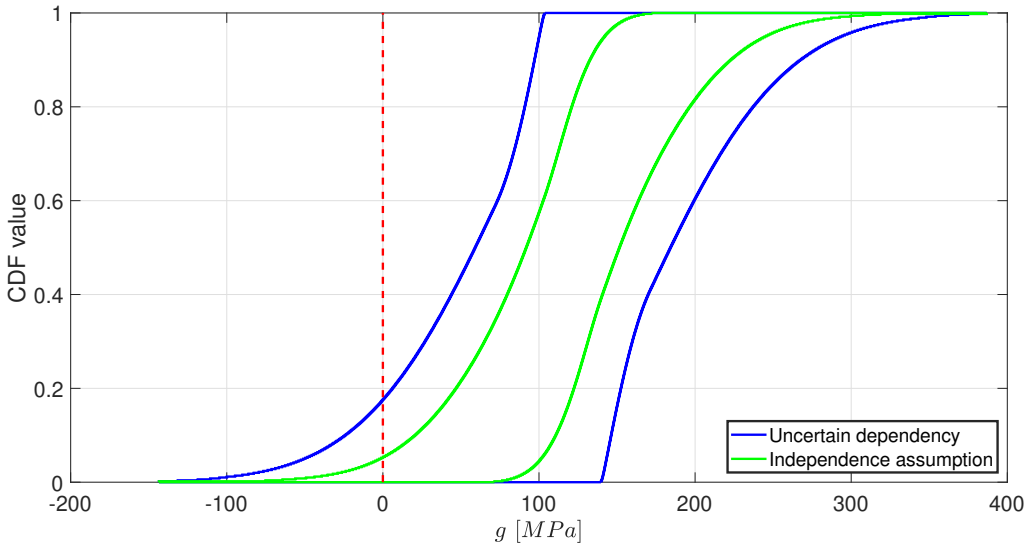

Figure 5: Resulting P-box obtained for the limit state function g. Note: The red dotted line denotes where $g = 0$.

	Uncertain dependency	Independence assumption
P_f	$[0, 0.1760]$	$[0, 0.0520]$

Table 4: Results to the uncertain P_f for the respective assumptions.

3.2.2 Sensitivity Analysis

The results of the sensitivity analysis via the Adaptive-pinching approach are summarised in Table 5. Based on the results, under both uncertain dependency and independence assumptions, the inferred parameter σ_S has consistently the highest value of sensitivity index. This implies that the aleatory variable S, particularly its standard deviation, contributes the most to the uncertainty on P_f which is consistent with the fact that there is less data on S. As such, there is a larger uncertainty on S compared to R.

In addition, it needs to be acknowledged that the uncertainty over the dependency between R and S also has significant contribution towards the uncertainty over P_f. As seen from the results in Table 4, there is a $70.45\ \%$ difference on the bounds on P_f between the consideration of uncertain dependencies and independence between the two aleatory variables.

$\boldsymbol{\theta}$	Uncertain dependency			Independence assumption		
	Ω	Pinched P_f	Rank	Ω	Pinched P_f	Rank
μ_R	0.1932	$[0, 0.1420]$	4	0.2692	$[0, 0.0380]$	3
σ_R	0.5000	$[0, 0.0880]$	2	0.2308	$[0, 0.0400]$	4
μ_S	0.4318	$[0, 0.1000]$	3	0.5769	$[0, 0.0220]$	2
σ_S	0.7727	$[0, 0.0400]$	1	0.9615	$[0, 0.0020]$	1

Table 5: Results to sensitivity index Ω and the ranking of the respective inferred parameters under the respective assumptions.

4 Challenge Problem 2

4.1 Problem Description

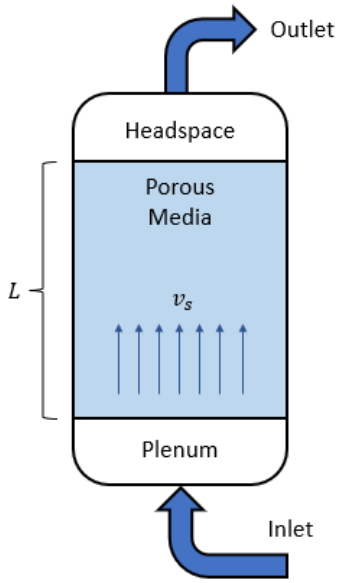

Figure 6: Schematic diagram of the reactor column set-up adopted from [4].

In this problem, a model reactor column is presented whose schematic diagram is illustrated in Figure 6. Without the consideration of mass and heat transfer, the pressure drop ΔP of the air flowing through the region of porous material is defined [4]:

$$\Delta P = \frac{150\mu L}{{D_p}^2} \cdot \frac{(1-\varepsilon)^2}{\varepsilon^3} \cdot \nu_s + \frac{1.75L\rho}{D_p} \cdot \frac{(1-\varepsilon)}{\varepsilon^3} \cdot {\nu_s}^2 \tag{8}$$

where D_p is the diameter of the porous media particles, ε is the porosity of the porous media, L is the length of the porous media, ρ is the density of fluid air set at $1.225\ kg/m^3$, mu is the dynamic viscosity of fluid air set at $1.81 \times 10^{-5}\ kg/m \cdot s$, and ν_s is the superficial velocity of fluid set at $0.35\ m/s$. The variables D_p, ε, and L are treated as aleatory variables whose respective data and corresponding ECDFs are presented in Table 6 and Figure 7 respectively. The failure probability P_f is defined as:

$$P_f = P(\Delta P > 15250Pa) \tag{9}$$

Based on the available information and data on D_p, ε, and L, the uncertainty on P_f needs to be quantified.

However, unlike in Challenge Problem 1 (i.e. see Section 3), there is no assumption on the form of distribution the aleatory variables follow, thereby introducing the element of model uncertainty to the problem. As such, this presents the need to perform a model selection on D_p, ε, and L. From there, PBA is implemented whilst also accounting for the uncertainty over the dependencies between D_p, ε, and L in the uncertainty quantification of P_f.

$D_p\ [m]$	0.0032	0.00395	0.0037	0.0035	0.0031	0.0040	0.0038	0.0038	0.0040	0.0037
$\varepsilon\ [-]$	0.375	0.347	0.329	0.352	0.388	0.419	0.404	0.394	0.352	0.370
$L\ [m]$	2.86	3.13	3.08	3.12	2.94	2.90	2.80	3.05	3.02	3.04

Table 6: Table of data for D_p, ε, and L.

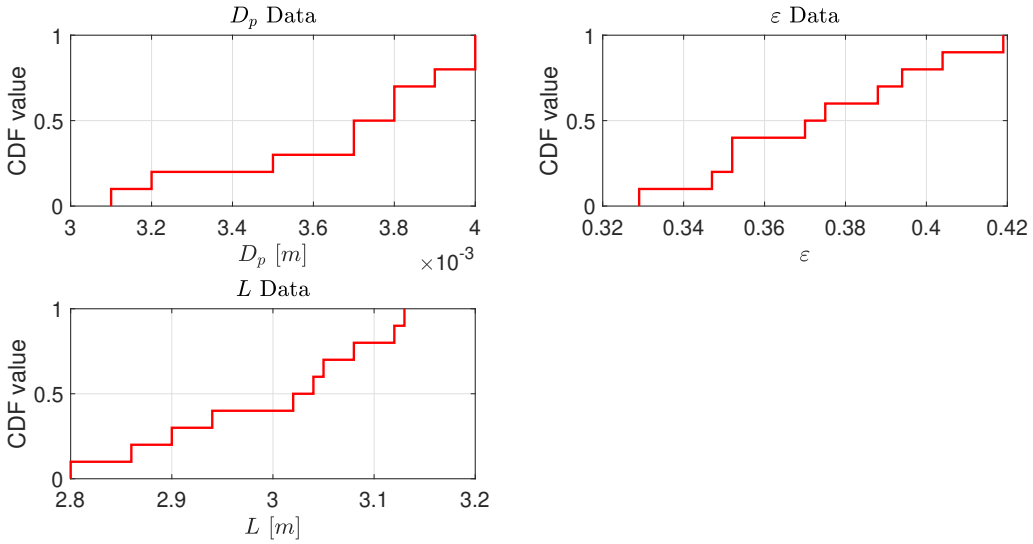

Figure 7: ECDF of D_p, ε, and L based on the numerical data in Table 6.

4.2 Results and Discussions

4.2.1 Model Calibration and Selection

Figure 7 presents the respective ECDF plots for the aleatory variables D_p, ε, and L. For each of the aleatory variables, two candidate distribution models M are considered: 1) Scaled Beta distribution; and 2) Normal distribution. The scaled Beta distribution is considered due to the flexibility in modelling the distribution shape to a certain degree of complexity using two shape parameters and it is defined as:

$$f_{Beta}(x) = \text{Beta}\left(\frac{x}{\gamma}; \alpha, \beta\right) \tag{10}$$

where γ is the scale factor corresponding to the maximum possible value of a given aleatory variable, while α and β are the shape parameters of the Beta distribution. To ensure a sufficiently finite support on each of the aleatory variables, the values of γ assigned to each of these variables are: 1) $\gamma = 0.005\ m$ for D_p; 2) $\gamma = 0.500$ for ε; and 3) $\gamma = 5.000\ m$ for L. The Normal distribution, on the other hand, is considered due to the physics-based assumption that it best describes the random errors in reality [15].

To determine the most probable distribution model M for each of the aleatory variable, the log model evidence $\log[P(\boldsymbol{D}|M)]$ is used as the metric. For each distribution model M, the Bayesian model updating approach is implemented to infer the corresponding shape parameters for D_p, ε, L:

- For the case of M being assigned a Scaled Beta distribution:
  $\boldsymbol{\theta}_{D_p} = \{\alpha_{D_p}, \beta_{D_p}\}$; $\boldsymbol{\theta}_{\varepsilon} = \{\alpha_{\varepsilon}, \beta_{\varepsilon}\}$; and $\boldsymbol{\theta}_{L} = \{\alpha_{L}, \beta_{L}\}$.

- For the case of M being assigned a Normal distribution:

  $\boldsymbol{\theta}_{D_p} = \{\mu_{D_p}, \sigma_{D_p}\}$; $\boldsymbol{\theta}_{\varepsilon} = \{\mu_{\varepsilon}, \sigma_{\varepsilon}\}$; and $\boldsymbol{\theta}_{L} = \{\mu_{L}, \sigma_{L}\}$.

Details to the respective inferred parameters are found in Tables 7 and 8.

For the likelihood function, the width parameter is set at $\epsilon = 5.0 \times 10^{-5}\ m$ for D_p, $\epsilon = 5.0 \times 10^{-3}$ for ε, and $\epsilon = 0.05\ m$ for L. The justification for this is as per presented in Section 3

$\boldsymbol{\theta}$	Description	Prior bounds	Units
α_{D_p}	Shape parameter 1 of D_p	$[0.01, 200]$	$[-]$
β_{D_p}	Shape parameter 2 of D_p	$[0.01, 200]$	$[-]$
α_{ε}	Shape parameter 1 of ε	$[0.01, 200]$	$[-]$
β_{ε}	Shape parameter 2 of ε	$[0.01, 200]$	$[-]$
α_{L}	Shape parameter 1 of L	$[0.01, 200]$	$[-]$
β_{L}	Shape parameter 2 of L	$[0.01, 100]$	$[-]$

Table 7: Details to the respective inferred parameters and the corresponding prior bounds given M assigned as the Scaled Beta distribution model.

$\boldsymbol{\theta}$	Description	Prior bounds	Units
μ_{D_p}	Mean of D_p	$[0.001, 0.005]$	$[m]$
σ_{D_p}	Standard deviation of D_p	$[0.0001, 0.0008]$	$[m]$
μ_{ε}	Mean of ε	$[0.01, 0.50]$	$[-]$
σ_{ε}	Standard deviation of ε	$[0.001, 0.080]$	$[-]$
μ_{L}	Mean of L	$[1.00, 5.00]$	$[m]$
σ_{L}	Standard deviation of L	$[0.010, 0.500]$	$[m]$

Table 8: Details to the respective inferred parameters and the corresponding prior bounds given M assigned as the Normal distribution model.

Due to the stochastic nature in the computation of $\log\left[P(\boldsymbol{D}|M)\right]$ by the TEMCMC sampling algorithm, 100 runs of computation is done for each of the aleatory variables for the corresponding choice of M. The resulting statistics of $\log\left[P(\boldsymbol{D}|M)\right]$ for each of the aleatory variable given each choice of M are presented in Table 9. Based on the results, it can be concluded that the most probable distribution model M for the respective aleatory variables are the following: 1) Normal distribution for D_p; 2) Normal distribution for ε; and 3) Scaled Beta distribution for L.

$\log\left[P(\boldsymbol{D}\|M)\right]$	D_p		ε		L	
	Beta	Normal	Beta	Normal	Beta	Normal
Mean	-8.6268	-8.5844	-7.2679	-7.1504	-5.0708	-5.4810
Standard deviation	0.4808	0.4011	0.4195	0.4707	0.2526	0.3116

Table 9: Resulting statistics of the log model evidence values for the corresponding aleatory variables given each choice of distribution model.

The resulting sample histogram obtained from $P(\boldsymbol{\theta}|\boldsymbol{D}, M)$ for the respective inferred parameters of the distribution model M for the corresponding aleatory parameters are presented in Figure 9. From which, credible intervals at different levels L_c could be obtained. The choice of L_c for the respective inferred parameters is presented in Table 10 to which the justification

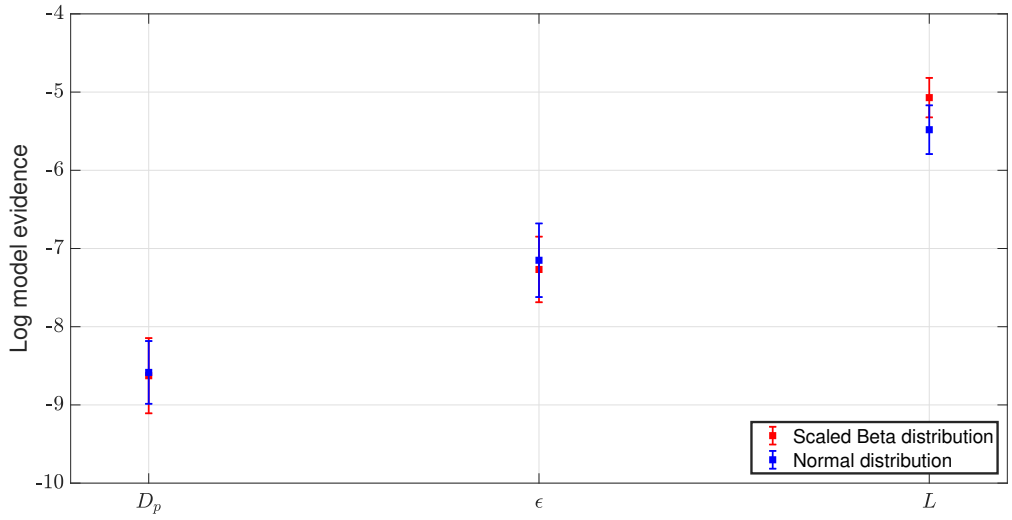

Figure 8: Resulting plots of the log model evidence results. The error-bars denote the 1-sigma bounds.

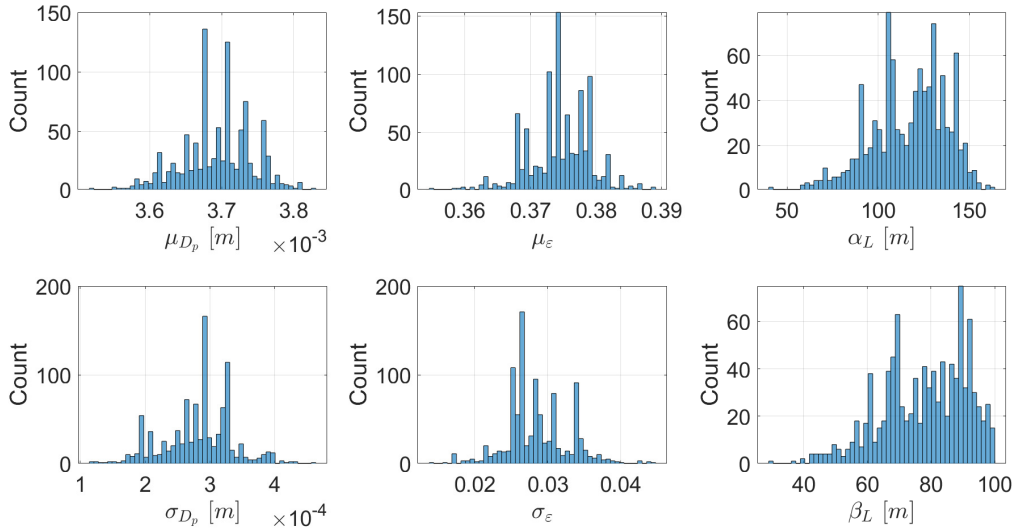

Figure 9: Histogram of the posterior samples for $\boldsymbol{\theta} = \{\mu_{D_p}, \sigma_{D_p}, \mu_\varepsilon, \sigma_\varepsilon, \alpha_L, \beta_L\}$.

$\boldsymbol{\theta}$	L_c [%]	Interval	Units
μ_{D_p}	0.0	$[3.5, 3.8] \times 10^{-3}$	$[m]$
σ_{D_p}	0.0	$[1.184, 4.634] \times 10^{-4}$	$[m]$
μ_ε	0.5	$[0.3604, 0.3866]$	$[-]$
σ_ε	0.5	$[0.0169, 0.0424]$	$[-]$
α_L	41.0	$[112.1297, 124.9070]$	$[-]$
β_L	41.0	$[75.1162, 83.7704]$	$[-]$

Table 10: Results to the L_c and the resulting interval for the respective inferred parameters.

is as per presented in Section 3. The resulting P-boxes for D_p, ε, and L are presented in Figure 10.

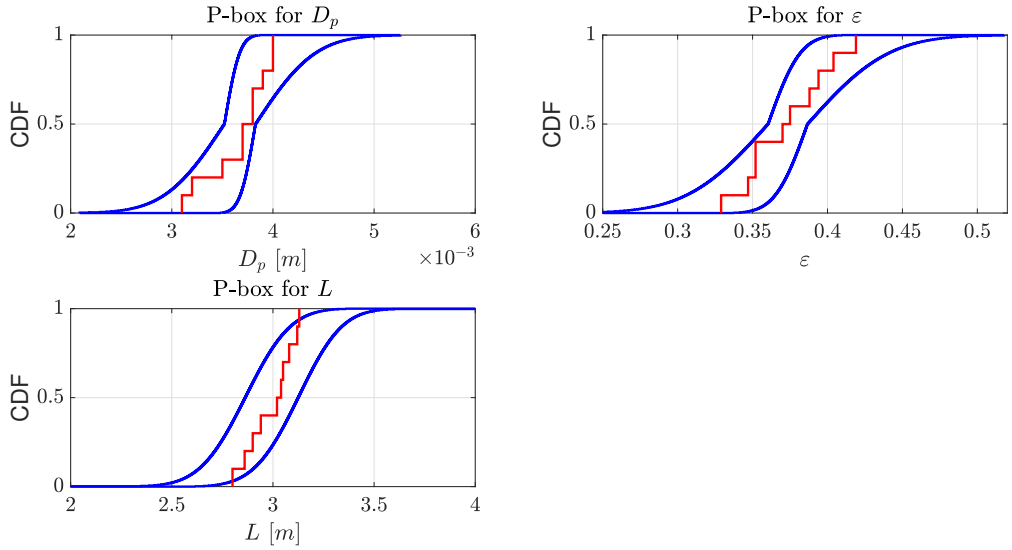

Figure 10: Resulting P-box obtained for D_p, ε, and L (in blue) along with their respective ECDFs of the observed data (in red).

From the resulting P-boxes obtained for D_p, ε, and L, the P-box for ΔP is obtained based on Eq. (8). Under different assumptions, the failure probability P_f is computed using Eq. (9) to which the results are presented in Table 11. From the table, it can be seen that there is a significant reduction in the P_f interval when independence between the aleatory variables is assumed. To provide a conservative yet robust decision on P_f, the resulting P_f interval under uncertain dependency between the aleatory variables and accounting for monotonicity of the variables is considered for this problem. Hence, the reference value will be set at $P_f = 0.1680$ which will be used for decision-making over the system in question. Figure 11 presents the resulting P-box plot for ΔP.

Assumption	P_f intervals
Independence	$[0, 0.0351]$
Uncertain dependency (Plain PBA)	$[0, 0.2860]$
Uncertain dependency (Considering monotonicity)	$[0, 0.1680]$

Table 11: Results to the uncertain P_f for the respective assumptions.

4.2.2 Sensitivity Analysis

The results of the sensitivity analysis via the Adaptive-pinching approach, accounting for the uncertainty over the dependency between the aleatory variables, are summarised in Table 12. Based on the results, the inferred parameter σ_ε has consistently the highest value of sensitivity index. This implies that the aleatory variable ε, particularly its standard deviation, contributes the most to the uncertainty on P_f. This is consistent with the fact that ε has the highest repetition in the formula for ΔP as seen in Eq. (8), therefore, making P_f more sensitive to the uncertainty of ε.

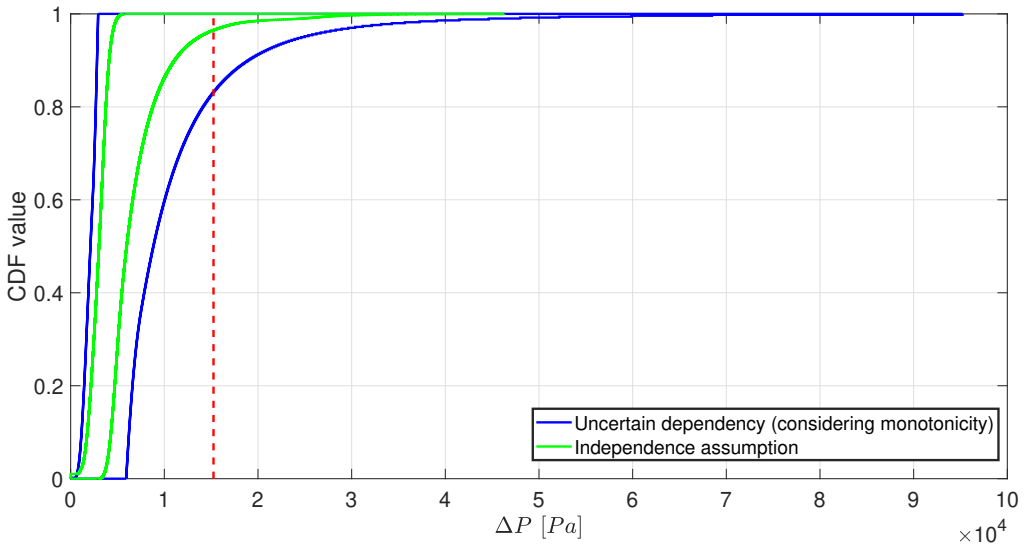

Figure 11: Resulting P-box obtained for the pressure drop ΔP. Note: The red dotted line denotes where $\Delta P = 15250\ Pa$.

$\boldsymbol{\theta}$	Uncertain dependency		
	Ω	Pinched P_f	Rank
μ_{D_p}	0.3095	$[0, 0.1160]$	4
σ_{D_p}	0.5952	$[0, 0.0680]$	2
μ_ε	0.5000	$[0, 0.0840]$	3
σ_ε	0.7619	$[0, 0.0400]$	1
μ_L	0.0595	$[0, 0.1580]$	6
σ_L	0.0714	$[0, 0.1560]$	5

Table 12: Results to sensitivity index Ω and the ranking of the respective inferred parameters under uncertain dependencies between the aleatory parameters.

5 Conclusion

The paper has presented numerous techniques which have been implemented to tackle the NAFEMS SWG Challenge. The Bayesian model updating technique is employed to: 1) perform probabilistic model updating on the distribution model used to characterise the distribution of the corresponding aleatory parameters under limited data; and 2) to infer the most probable distribution model on the available data under model uncertainty through the use of the Transitional Ensemble Markov Chain Monte Carlo sampler [8].

To quantify the uncertainty over the failure probability, Probability Bounds Analysis is used to construct a P-box on a performance function given the P-box constructed for the aleatory variables using Bayesian model updating. The robust computation of the interval bounds on the failure probability does not assume independence on the aleatory variables, but rather accounts for the uncertainty over the dependencies between these variables.

To perform the Sensitivity analysis on the distribution parameters and from there, determine the aleatory variable whose uncertainty contributes the most to the uncertainty of the failure probability, the adaptive pinching method is employed [12]. Such method serves to provide a non-empirical method for pinching and to indirectly quantify the sensitivity of the aleatory variable by pinching the interval of its distribution parameters. From which, the maximum sen-

sitivity index is computed and used to rank and determine the most sensitive aleatory variable.

To provide the readers with a greater understanding of the numerical methods implemented as well as to reproduce the results presented in the paper, the MATLAB codes used to perform Bayesian model updating as well as the R codes used to perform the Probabilistic Bounds Analysis are made accessible via: `https://github.com/Institute-for-Risk-and-Uncertainty/NAFEMS-UQ-Challenge-2022`

REFERENCES

[1] C. J. Roy and W. L. Oberkampf, "A comprehensive framework for verification, validation, and uncertainty quantification in scientific computing," *Computer Methods in Applied Mechanics and Engineering*, vol. 200, pp. 2131–2144, 2011.

[2] W. L. Oberkampf, J. C. Helton, C. A. Joslyn, S. F. Wojtkiewicz, and S. Ferson, "Challenge problems: Uncertainty in system response given uncertain parameters," *Reliability Engineering and System Safety*, vol. 85, pp. 11–19, 2004.

[3] A. D. Kiureghian and O. Ditlevsen, "Aleatory or epistemic? Does it matter?," *Structural Safety*, vol. 31, pp. 105–112, 2009.

[4] NAFEMS, "Uncertain knowledge: A challenge problem." Available at `https://www.nafems.org/community/working-groups/stochastics/challenge_problem/` (2022).

[5] A. Lye, A. Cicirello, and E. Patelli, "A Review of Stochastic Sampling Methods for Bayesian Inference Problems," *In Proceedings of the 29th European Safety and Reliability Conference*, vol. 1, pp. 1866–1873, 2019.

[6] A. Lye, A. Cicirello, and E. Patelli, "Sampling methods for solving Bayesian model updating problems: A tutorial," *Mechanical Systems and Signal Processing*, vol. 159, 2021.

[7] J. Ching and Y. C. Chen, "Transitional Markov Chain Monte Carlo Method for Bayesian Model Updating, Model Class Selection, and Model Averaging," *Journal of Engineering Mechanics*, vol. 133, 2007.

[8] A. Lye, A. Cicirello, and E. Patelli, "An efficient and robust sampler for Bayesian inference: Transitional Ensemble Markov Chain Monte Carlo," *Mechanical Systems and Signal Processing*, vol. 167, p. 108471, 2022.

[9] B. M. Turner and T. V. Zandt, "A tutorial on approximate Bayesian computation," *Journal of Mathematical Psychology*, vol. 56, no. 2, pp. 69–85, 2012.

[10] S. Bi, M. Broggi, and M. Beer, "The role of the Bhattacharyya distance in stochastic model updating," *Mechanical Systems and Signal Processing*, vol. 117, pp. 437–452, 2019.

[11] M. de Angelis and A. Gray, "Why the 1-wasserstein distance is the area between the two marginal cdfs," 2021.

[12] A. Lye, M. Kitahara, M. Broggi, and E. Patelli, "Robust optimization of a dynamic Black-box system under severe uncertainty: A distribution-free framework," *Mechanical Systems and Signal Processing*, vol. 167, p. 108522, 2022.

[13] A. Gray, A. Wimbush, M. D. Angelis, P. O. Hristov, D. Calleja, E. Miralles-Dolz, and R. Rocchetta, "From inference to design: A comprehensive framework for uncertainty quantification in engineering with limited information," *Mechanical Systems and Signal Processing*, vol. 165, p. 108210, 2022.

[14] N. Gray, S. Ferson, M. De Angelis, A. Gray, and F. B. de Oliveira, "Probability bounds analysis for python," *Software Impacts*, vol. 12, p. 100246, 2022.

[15] NIST, "The random errors follow a normal distribution." Available at https://www.itl.nist.gov/div898/handbook/pmd/section2/pmd214.htm (2022).